



HAL
open science

Laser induced ultrafast 3d and 4f spin dynamics in CoDy ferrimagnetic alloys as a function of temperature

Tom Ferté, Grégory Malinowski, Erwan Terrier, Valérie Halté, L Le Guyader, Karsten Holldack, Michel Hehn, Christine Boeglin, Nicolas Bergéard

► To cite this version:

Tom Ferté, Grégory Malinowski, Erwan Terrier, Valérie Halté, L Le Guyader, et al.. Laser induced ultrafast 3d and 4f spin dynamics in CoDy ferrimagnetic alloys as a function of temperature. *Journal of Magnetism and Magnetic Materials*, 2021, 530, pp.167883. 10.1016/j.jmmm.2021.167883. hal-03420828

HAL Id: hal-03420828

<https://hal.science/hal-03420828>

Submitted on 9 Nov 2021

HAL is a multi-disciplinary open access archive for the deposit and dissemination of scientific research documents, whether they are published or not. The documents may come from teaching and research institutions in France or abroad, or from public or private research centers.

L'archive ouverte pluridisciplinaire **HAL**, est destinée au dépôt et à la diffusion de documents scientifiques de niveau recherche, publiés ou non, émanant des établissements d'enseignement et de recherche français ou étrangers, des laboratoires publics ou privés.



Distributed under a Creative Commons Attribution - NonCommercial - NoDerivatives 4.0 International License

1 Title: **Laser induced ultrafast 3d and 4f spin dynamics in CoDy ferrimagnetic alloys as a**
2 **function of temperature.**

3
4 T. Ferté¹, G. Malinowski², E. Terrier¹, V. Halté¹, L. Le Guyader³, K. Holldack³, M. Hehn², C.
5 Boeglin¹ and N. Bergeard^{1*}

6
7 ¹ *Université de Strasbourg, CNRS, Institut de Physique et Chimie des Matériaux de Strasbourg,*
8 *UMR 7504, F-67000 Strasbourg, France.*

9
10 ² *Institut Jean Lamour, Université de Lorraine, BP 50840, 54011 Nancy, France*

11
12 ³ *Institut für Methoden und Instrumentierung der Forschung mit Synchrotronstrahlung*
13 *Helmholtz-Zentrum Berlin für Materialien und Energie GmbH, Albert-Einstein-Str. 15, 12489*
14 *Berlin, Germany*

15
16 * *Corresponding author:*

17 *Mel: nicolas.bergeard@ipcms.unistra.fr*

18 *Address: Institut de Physique et de Chimie des Matériaux de Strasbourg (IPCMS)*
19 *Campus Cronenbourg 23 rue du Loess BP43 67034 Strasbourg*

20
21 **0. Abstract**

22
23 We report an element- and time-resolved investigation of femtosecond laser induced
24 ultrafast dynamics of the Co 3d and Dy 4f spins in a ferrimagnetic Co₈₀Dy₂₀ alloy as a function
25 of the temperature. We observe that the Co characteristic demagnetization time (τ_{Co}) remains
26 nearly constant (~ 0.2 ps) on increasing the temperature. Conversely, the Dy characteristic
27 demagnetization time (τ_{Dy}) decreases from ~ 1 ps to ~ 0.4 ps with the rise of temperature.
28 Comparing our experimental data with literature shows that τ_{Co} and τ_{Dy} are independent of the
29 alloy composition or the demagnetization amplitude and that τ_{Dy} scales with the relative
30 temperature $T^* = T_{\text{Curie}} - T$.

31
32 *Key words:*

33 **Ferrimagnetic alloys, ultrafast laser induced demagnetization, femtosecond laser, time-**
34 **resolved X-ray Magnetic Circular Dichroism.**

35 Highlights:

- 36 • Element- and time-resolved investigation of laser induced ultrafast Co3d and Dy4f spin
37 dynamics in a ferrimagnetic CoDy amorphous alloy as a function of temperature.
38
- 39 • The Co characteristic demagnetization time remains nearly constant (~0.2 ps) on
40 increasing the temperature while the Dy characteristic demagnetization time decreases
41 from ~1 ps to ~0.4 ps with the rise of temperature.
42

43 **1. Introduction**

44

45 Excitation of ferromagnetic layers with infra-red (IR) femtosecond (fs) laser pulses leads to
46 a quenching of the magnetic order on a sub-picosecond time scale [1]. The microscopic
47 mechanisms governing this ultrafast demagnetization are still subject to controversy in spite of
48 intensive experimental and theoretical studies [2 - 8]. Although these investigations have
49 revealed fundamental dissimilarities in the laser induced ultrafast magnetization dynamics in
50 transition metals (TM) [1, 9 - 11] and in rare-earth (RE) films [12 - 16], a few general features
51 were established. For instance, a rise in temperature results in an increase of the characteristic
52 quenching times (τ) of the 3d magnetic order in pure transition metals (TM) and 5d magnetic
53 order in pure rare-earth (RE) films [11, 13, 17]. In the specific case of pure RE layers, such
54 behaviour is also expected for the localized 4f spins as theoretically predicted [13] and sustained
55 by experiments that have evidenced concomitant laser induced dynamics of the 5d and 4f spins
56 [12 - 14, 16, 18]. In these experiments, the IR fs laser pulses excite the RE 5d spins while the
57 RE 4f spin dynamics is indirectly triggered via the 5d-4f intra-atomic exchange coupling [12,
58 14].
59

60 In RE-TM ferrimagnetic alloys, the RE 4f spin order originates from the Ruderman-Kittel-
61 Kasuya-Yosida (RKKY) exchange coupling [19]. The RE 4f – RE 4f indirect exchange coupling
62 is mediated by the RE 5d as well as the TM 3d electrons in the conduction band [20].
63 Interestingly, the published element- and time-resolved experiments have reported distinct laser
64 induced ultrafast dynamics for the TM 3d and RE 4f spins in spite of this RKKY exchange
65 coupling [21 – 30]. Recently, the Landau-Lifshitz-Bloch (LLB) model [13, 17] was extended
66 to treat the laser induced ultrafast dynamics in multi-sublattices ferrimagnetic alloys [31] such
67 as FeCoGd [32], CoTb [33] and FeTb [34] alloys. The calculations based on this modified LLB

68 model have shown that the characteristic demagnetization times of both the FeCo (τ_{FeCo}) and
69 the Gd (τ_{Gd}) sublattices in FeCoGd alloys strongly depend on the difference between the initial
70 temperature (T) and the Curie temperature (T_{Curie}) of the alloy [32]. This theoretical work
71 highlights explicitly the differences between the ultrafast laser induced TM 3d and the RE 4f
72 spin dynamics in these alloys with the variation of the temperature [32]. Hennecke et al. have
73 invoked the effect of temperature to explain the short Gd demagnetization time they have
74 evidenced in a FeCoGd alloy [30]. Ferté et al. have earlier investigated the laser induced
75 demagnetization in $\text{Co}_{80}\text{Dy}_{20}$ and $\text{Co}_{78}\text{Dy}_{22}$ alloys at different initial temperatures but ensuring
76 a constant relative temperature $T_{\text{Curie}} - T$ [27]. They have shown that the response of the Dy
77 (resp. Co) magnetization to laser excitation was the same for both alloys in line with the LLB
78 calculations. The distinct dynamics of 3d and 4f spins is believed to be the key ingredient for
79 ultrafast all optical switching [21, 35] as well as ultrafast spin-transfer torque assisted switching
80 [36] in RE-TM alloys. Thus, it is of paramount importance to determine the correlation between
81 the characteristic demagnetization times and physical parameters such as the temperature.
82 However, systematic element- and time-resolved investigations of laser induced spin dynamics
83 in a single RE-TM alloy as a function of temperature are still lacking.

84

85 In this work, we have studied the laser induced ultrafast dynamics of Co3d and Dy4f spins
86 in a $\text{Co}_{80}\text{Dy}_{20}$ ferrimagnetic alloy as a function of temperature by mean of time-resolved X-Ray
87 Magnetic Circular Dichroism (tr-XMCD) [37]. Interestingly, we report experimental evidences
88 that the dependence of the laser induced dynamics of Co 3d and Dy 4f spins on temperature are
89 clearly different. We observe that τ_{Co} remains nearly constant (~ 0.2 ps) while τ_{Dy} decreases from
90 ~ 1 ps to ~ 0.4 ps when the temperature rises from 160K to 350K. Furthermore, a comparison of
91 our experimental data with existing data from literature on laser induced ultrafast dynamics of
92 Dy 4f spins in CoDy alloys [25, 27] suggests that τ_{Dy} is determined by $T^* = T_{\text{Curie}} - T$.

93

94 **2. Material and methods**

95

96 The 18 nm thick $\text{Co}_{80}\text{Dy}_{20}$ alloy layer was deposited by DC magnetron sputtering on a “heat
97 sink” Ta(3)/Cu(20)/Ta(3) multilayer sustained by a Si_3N_4 membrane. The alloy was capped with
98 a Al(3)/Ta(3) bi-layer to prevent oxidation. The $\text{Co}_{80}\text{Dy}_{20}$ alloy displays an out-of-plane
99 magnetic anisotropy. We have recorded hysteresis loops at various temperatures using SQUID
100 magnetometry to extract the dependence of the coercive field (H_C) on temperature. For these

101 measurements, we have used a test $\text{Co}_{80}\text{Dy}_{20}$ alloy layer deposited simultaneously with the one
102 used for the time-resolved experiments but on a Si substrate (figure 1). This figure shows a
103 divergence of H_C in the vicinity of $T \sim 250\text{K}$ indicating the temperature of magnetic
104 compensation [38, 39].

105

106 The tr-XMCD experiments were carried out at the femtoslicing beam line of the BESSY II
107 synchrotron radiation source at the Helmholtz-Zentrum Berlin [37]. The magnetization
108 dynamics have been measured by monitoring the transmission of circularly polarized X-ray
109 pulses tuned to specific core level absorption edges as a function of a pump-probe delay for two
110 opposite directions of the magnetic field. The photon energy was set to the CoL_3 and the DyM_5
111 edges using a reflection zone plate monochromator on UE56/1-ZPM. The full width at half
112 maximum (FWHM) of the 800nm pump laser was set to $500 \mu\text{m}$ to ensure homogeneous
113 pumping over the probed area of the sample (FWHM $\sim 200 \mu\text{m}$). A magnetic field of $\pm 0.55 \text{ T}$
114 was applied along the propagation axis of both the IR laser and the X-ray beam during the
115 experiment. The measurements were carried out at $T^* = 350 \text{ K}$ (configuration 1), 400 K
116 (configuration 2) and 540 K (configuration 3) with $T^* = T_{\text{Curie}} - (T_{\text{cryo}} + \Delta T)$ as illustrated in
117 figure 2. Here, T_{cryo} is the temperature of the cryostat and ΔT is the temperature elevation due
118 to the continuous laser heating (table 1). The Curie temperature of the $\text{Co}_{80}\text{Dy}_{20}$ alloy ($T_{\text{Curie}} =$
119 700 K) is extrapolated from literature [40] and from mean field calculations [41, 42]. As only
120 one single sample was used in this experiment, any small error on the estimated value of T_{Curie}
121 would shift T^* without affecting our conclusions. We have determined that the coercive field
122 of the $\text{Co}_{80}\text{Dy}_{20}$ alloy was below 0.55 T either below 160 K or above 300 K by monitoring the
123 XMCD amplitude as a function of temperature. The divergence of H_C between 160 K and 300
124 K is related to $T_{\text{comp}} \sim 250 \text{ K}$ as illustrated in figure 1. As a consequence, the experimental
125 parameters, such as the pump laser powers (P) and T_{cryo} , have been chosen so that $T_{\text{cryo}} + \Delta T$
126 stay in the temperature ranges that allow for magnetic saturation of our alloy. We have relied
127 on the thermal variation of the coercive field to determine ΔT for the two different pump laser
128 powers ($P = 17$ and 50 mW) that we have used during the experiment. To do so, we initially set
129 $T_{\text{cryo}} = 80 \text{ K}$ and turned on the laser. $P = 17 \text{ mW}$ was the largest laser power for which $T_{\text{cryo}} +$
130 ΔT stays below $T = 160\text{K}$. Above this temperature, the CoDy alloy could not be saturated. As a
131 consequence, we estimated that $\Delta T \sim 80 \text{ K}$ for $P = 17\text{mW}$. In order to estimate ΔT with $P = 50$
132 mW , we compared the hysteresis loops at $T_{\text{cryo}} = 300$ and 320 K with $P = 0 \text{ mW}$ to the hysteresis
133 loops recorded at negative delay for $T_{\text{cryo}} = 80\text{K}$ with $P = 50 \text{ mW}$ (figure 3). The same signs of
134 the hysteresis loops indicate that these measurements were performed above T_{comp} . Moreover,

135 we notice that the coercive field is smaller for $P = 50\text{mW}$ and $T_{\text{cryo}} = 80\text{K}$ compared to $P = 0$
136 mW and $T_{\text{cryo}} = 300$ and 320 K. According to the thermal variation of the saturation field above
137 T_{comp} (figure 1), we estimated that $T_{\text{cryo}} + \Delta T$ is above 320K for $P = 50\text{mW}$ and $T_{\text{cryo}} = 80\text{K}$.
138 The shape of the hysteresis loop at $P = 50\text{mW}$ and $T_{\text{cryo}} = 80\text{K}$ also indicates that we are close
139 to the temperature of spin reorientation transition [43]. As a consequence, we estimated $\Delta T >$
140 250 K for $P = 50$ mW. Our procedure to estimate ΔT results in significant error bars on T^*
141 (figure 5). Nevertheless, we estimated that we performed the time-resolved experiments at T^*
142 $= 350$ K, 400 K and 540 K (figure 2, table 1). The measurements were carried out above T_{comp}
143 for the configurations 1 and 2 (figure 2a and b) and below T_{comp} for the configurations 3 (figure
144 2c) [27].

145

146 **3. Experimental results and discussion**

147

148 The normalized transient XMCD signals recorded at the Co L_3 and Dy M_5 edges for $T^* =$
149 350 , 400 and 540 K are displayed in figure 4a, b and c respectively. At $T^*=540\text{K}$ (figure 4c),
150 the maximum demagnetization of the Co sublattice is reached while the demagnetization of the
151 Dy sublattice has barely started as reported in a large number of element- and time-resolved
152 experiments for different RE-TM alloys [21 - 27]. In contrast, at $T^* = 350\text{K}$ (figure 4a), the
153 magnetization of the Dy sublattice is close to its minimum value while the minimum
154 magnetization of the Co sublattice is reached. The tr-XMCD curves at the Co L_3 edges were
155 fitted with two exponential functions (respectively the demagnetization and the magnetization
156 recovery) convoluted with a Gaussian function which account for the experimental time
157 resolution (130 fs) [24, 44, 45]. It is worth noticing that we have imposed a lower limit at 130
158 fs for the characteristic demagnetization times during the fitting procedure. It means that the
159 actual τ_{Co} is possibly below the experimental time resolution for $T^* = 400$ K and 540K . The tr-
160 XMCD curves at the Dy M_5 edge were adjusted by a single exponential decay convoluted by a
161 Gaussian function since we did not observe any recovery on the recorded time range. We have
162 extracted the characteristic demagnetization times (τ) from these fits as well as their error bars,
163 which correspond to one standard deviation (table 1). The dependence of the characteristic
164 demagnetization times on temperature for both sublattices are displayed in figure 5. We also
165 report the characteristic demagnetization times for the Co and Dy sublattices in various CoDy
166 alloys measured by Ferté et al (in $\text{Co}_{80}\text{Dy}_{20}$ and $\text{Co}_{78}\text{Dy}_{22}$) [27] and Radu et al (in $\text{Co}_{83}\text{Dy}_{17}$)
167 [25] in figure 6. Ferté et al have explicitly given the numerical values for T_{cryo} , T_{Curie} and ΔT

168 [27] and therefore we have derived $T^* = 430$ and 450K for the $\text{Co}_{80}\text{Dy}_{20}$ and $\text{Co}_{78}\text{Dy}_{22}$ alloys
 169 respectively. Radu et al have performed their measurements at $T = 100\text{K}$ without considering
 170 any DC heating. Therefore, we assume $\Delta T = 0\text{K}$ and we include an extended error bar for this
 171 data. It is worth noticing that including a temperature elevation of $\Delta T \sim 100\text{-}200\text{ K}$ (typical
 172 values estimated for the pump-probe experiments on thin films) will not change our main
 173 message. Thus, we derived $T^*=930\text{K}$ since $T_{\text{Curie}} = 1030\text{K}$ for their $\text{Co}_{83}\text{Dy}_{17}$ alloys [43].

174
 175 *Table 1: Characteristic demagnetization times extracted from the fit functions as a function of*
 176 *temperature T^* . The cryostat temperature (T_{cryo}), the laser continuous heating (ΔT), the laser*
 177 *power and the X-ray absorption edges are also recalled.*

T^* (K)	T_{Cryo} (K)	ΔT (K)	Laser power (mW)	Edge	Demagnetization time τ (fs)
540	80	80	17	Co L_3	130 ± 100
540	80	80	17	Dy M_5	980 ± 200
400	220	80	17	Co L_3	130 ± 60
400	220	80	17	Dy M_5	570 ± 90
350	80	> 250	50	Co L_3	212 ± 25
350	80	> 250	50	Dy M_5	400 ± 100

178
 179 In figure 5, we observe that τ_{Co} is almost constant within the error bars between $T^* =$
 180 350 K and $T^* = 540\text{K}$ in spite of the various laser powers used, and thus the different
 181 demagnetization amplitudes, in line with previous work by Jal et al [46]. We also observe a
 182 clear decrease of τ_{Dy} when T^* decreases from 540K to 350K (figure 5). In pure Gd layers, the
 183 characteristic demagnetization time τ_{Gd} related to the (5d, 6s) magnetic order increases when
 184 the laser power is increased [13, 16]. The concomitant quenching of itinerant (5d, 6s) and
 185 localized 4f magnetic order in pure RE layers [12 - 16, 18, 47] suggests that such an increase is
 186 also expected for the 4f spins. However, such a behavior is not observed in our CoDy alloy
 187 since the shorter demagnetization time (τ_{Dy}) is obtained for the larger laser power ($P = 50\text{mW}$)
 188 and thus also for the larger demagnetization amplitude. Therefore, we can rule out the distinct
 189 laser power as the origin of the measured variation of τ_{Dy} with temperature. Gang et al. have
 190 reported a decrease of the Ni 3d characteristic demagnetization time in NiPd ferromagnetic

191 alloys when the Curie temperature is reduced (and thus T^*) by increasing the Pd concentration
192 [48]. They have attributed such feature to an increase of the spin-flip scattering probability [2]
193 with Pd content, caused by its larger spin-orbit coupling compared to pure Ni. In our case, this
194 explanation does not hold since we have studied a single alloy composition. According to the
195 LLB calculations in ferrimagnets [32], by increasing the temperature, we would expect to go
196 from a situation in which $\tau_{TM} < \tau_{RE}$ at low temperatures ($T \ll T_{Curie}$) to a situation in which τ_{TM}
197 $\sim \tau_{RE}$ at higher temperatures ($T > 0.8 T_{Curie}$). The transition between these dynamical regimes
198 requires that τ_{Dy} decreases and/or τ_{Co} increases in the intermediate temperature range. Our
199 experimental findings are thus consistent with this LLB prediction but call for further
200 experiments at even higher temperatures, especially in the vicinity of T_{Curie} to challenge further
201 their predictions.

202

203 Two qualitative descriptions can be proposed to explain the different temperature
204 dependent evolution of τ_{Co} and τ_{Dy} . The first one considers that different microscopic
205 mechanisms are supposed to be responsible for the laser induced ultrafast quenching of Co 3d
206 and Dy 4f magnetic orders. Indeed, the dynamics of TM 3d spins is presumably caused by spin-
207 flip scattering [49 - 51] and superdiffusive spin transport [3, 52] while the dynamics of the RE
208 4f spins is claimed to be related to spin-waves [53 - 55]. The second one considers that the Co
209 3d spin dynamics is mainly governed by the direct ferromagnetic Co – Co exchange coupling
210 while the Dy 4f spin dynamics is mainly governed by the indirect antiferromagnetic Co – Dy
211 exchange coupling. Recent measurements have shown that antiferromagnetic and
212 ferromagnetic materials exhibit distinct laser induced ultrafast dynamics [56].

213

214 Finally, in figure 6, we compare our experimental results with existing data from the
215 literature [31, 33] by plotting τ_{Co} and τ_{Dy} as a function of T^* for different alloy compositions.
216 We observe that τ_{Co} and τ_{Dy} are both constant (within error bars) from $T^* = 930$ K to $T^* = 540$
217 K. From $T^* = 540$ K to $T^* = 350$ K, we observe that τ_{Co} is constant while τ_{Dy} decreases,
218 confirming our experimental results from figure 5. It is also very interesting to note that the τ_{Dy}
219 extracted from the work of Ferté et al. are consistent with our present results for similar T^*
220 although in their case the demagnetization amplitudes were larger than 80%. It suggests that
221 τ_{Dy} does not depend on the demagnetization amplitude but mainly on $T^* = T_{Curie} - T$.

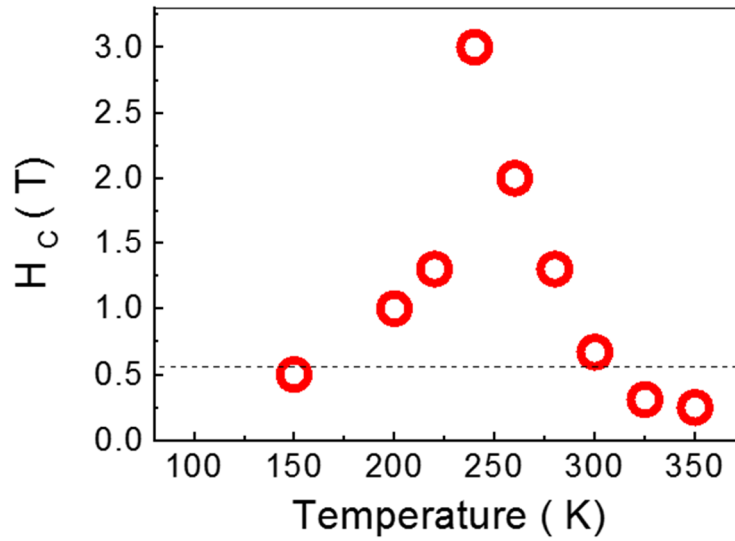
222

223 **4. Conclusions**

224

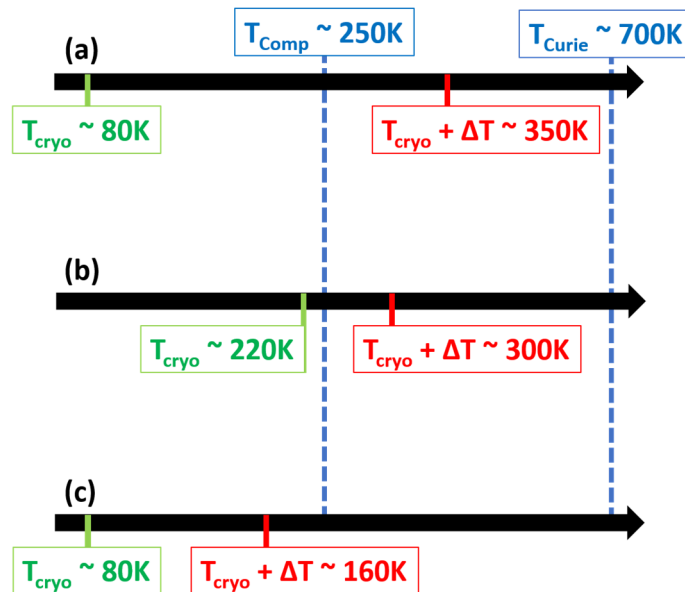
225 We have investigated the laser induced ultrafast dynamics of Co 3d and Dy 4f spins in a
226 ferrimagnetic CoDy alloy as a function of temperature by element- and time-resolved XMCD.
227 We have revealed striking differences between the Co 3d and Dy 4f spin dynamics when the
228 temperature is varying from 160 K to 350K. The characteristic demagnetization time of the
229 Dy4f sublattice decreases while it is almost constant for the Co3d sublattice. This experimental
230 findings sustain some of the predictions of the LLB model, namely that the characteristic
231 demagnetization time of the RE sublattice should be smaller than that of the TM sublattice at
232 high temperature. Our experimental results also confirm that the characteristic demagnetization
233 time of the Co sublattice does not depend on the composition, on the demagnetization amplitude
234 nor on the temperature in CoDy alloys as reported by Jal et al [46]. Finally, our data set,
235 amended with data extracted from literature, suggest that the characteristic demagnetization
236 time of the Dy sublattice is determined by $T^* = T_{\text{Curie}} - T$ and does not depend on the
237 demagnetization amplitude or alloy composition. Our work calls for further experimental
238 investigations at elevated temperatures to challenge the predictions of the LLB model for spin
239 dynamics in RE-TM alloys, especially in the vicinity of T_{Curie} . Such experimental confirmation
240 would link the characteristics of laser induced ultrafast dynamics and the static magnetic
241 properties of ferrimagnetic alloys [32]. We hope this work will motivate further experimental
242 investigation at elevated temperatures as well as development of the LLB model to
243 ferrimagnetic alloys [57].

244
245 **Figures:**

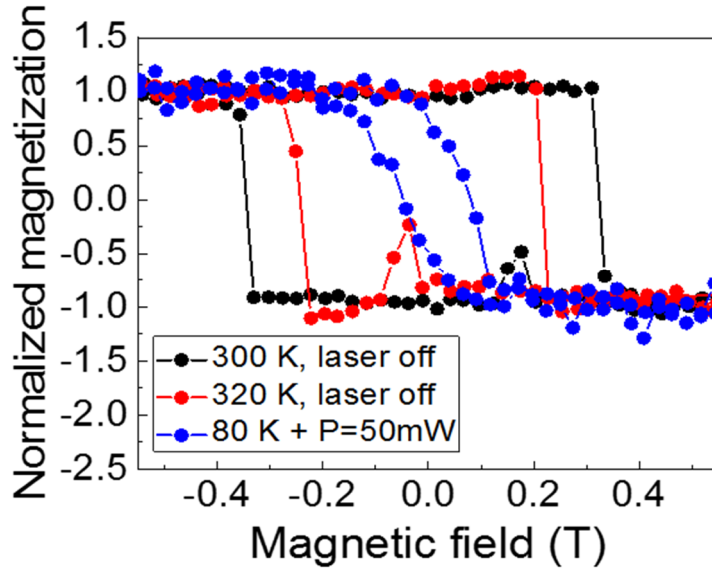


246
247
248 *Figure 1: Dependence of the coercive field (H_C) on the temperature for a $Co_{80}Dy_{20}$ alloy measured by means of*
249 *SQUID magnetometry (red empty circles). H_C diverges in the vicinity of $T \sim 250K$ defining the temperature of*
250 *magnetic compensation ($T_{comp} \sim 250K$). The horizontal dotted line corresponds to $H = 0.55 T$ which is the maximum*
251 *magnetic field available on the femtoslicing end-station [37]. The $Co_{80}Dy_{20}$ alloy layer used for SQUID*
252 *measurements was deposited simultaneously with the one used for the time-resolved experiments deposited on*
253 *transparent SiN membrane.*

254

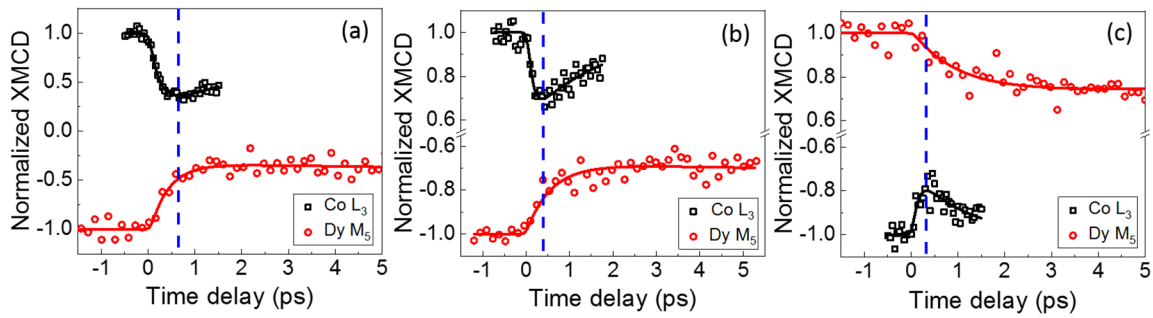


255
256
257 *Figure 2: Sketch of the experimental conditions to achieve our different relative temperatures $T^* = T_{Curie} - (T_{cryo} -$*
258 *$\Delta T) = 350K$ (a), $400K$ (b) and $540K$ (c).*



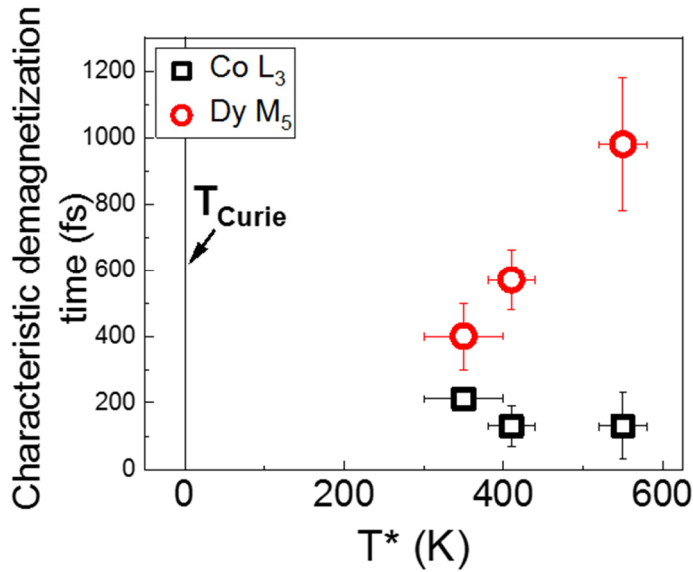
259
260
261
262
263

Figure 3: Hysteresis loops recorded by monitoring the X-ray transmission at the Dy M_5 absorption edge as a function of the magnetic field. The experimental configurations were $P = 0mW$ and $T_{cryo} = 300K$ (black circles), $P = 0mW$ and $T_{cryo} = 320K$ (red circles) and $P = 50mW$ and $T_{cryo} = 80K$ (black circles).



264
265
266
267
268

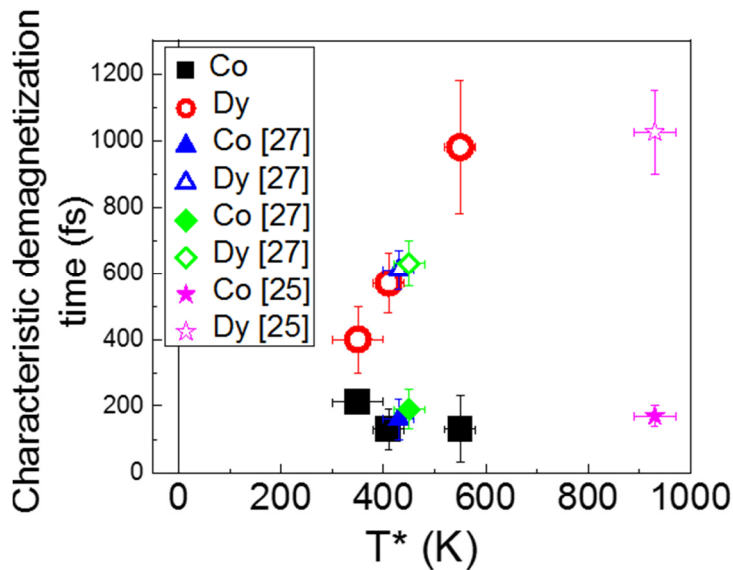
Figure 4: Transient XMCD at the Co L_3 (black squares) and Dy M_5 (red circles) edges as a function of the pump – probe delay measured at $T^* = 350 K$ (a), $400 K$ (b) and $540 K$ (c). The solid lines are the fitting functions. The vertical blue dotted lines denote the delay at which the magnetization of the Co sublattices reaches the minimal value.



269

270 *Figure 5: Characteristic demagnetization times for Co (black squares) and Dy (red circles) sublattices as a*
 271 *function of T^* . The error bars on the characteristic demagnetization times is given by the standard deviation from*
 272 *the fitting function. The error bars on the temperature were experimentally estimated (details in the text).*

273



274

275 *Figure 6: Characteristic demagnetization times for Co (filled symbols) and Dy (open symbols) sublattices as a*
 276 *function of T^* . We report our experimental results (black squares and red circles) superposed to published data*
 277 *extracted from element and time-resolved experiments performed on $Co_{80}Dy_{20}$ (filled and empty blue triangles)*
 278 *[27], $Co_{78}Dy_{22}$ (filled and empty green lozenges) [27] and $Co_{83}Dy_{17}$ (filled and empty magenta stars) [25].*

279

280

281 **Acknowledgments:**

282

283 We thank HZB for the allocation of synchrotron radiation beamtime. We are indebted for the
 284 scientific and technical support given by N. Pontius, Ch. Schüßler-Langeheine and R. Mitzner
 285 at the slicing facility at the BESSY II storage ring. We thank D. Gupta for a careful reading and

286 her suggestions to improve the manuscript. This project has received funding from the European
287 Union's Horizon 2020 research and innovation programme under grant agreement No 730872.
288 The authors are grateful for financial support received from the following agencies: the French
289 “Agence National de la Recherche” via Project No. ANR-11-LABX-0058_NIE and Project
290 EQUIPEX UNION No. ANR-10-EQPX-52, the CNRS-PICS program, the EU Contract
291 Integrated Infrastructure Initiative I3 in FP6 Project No. R II 3CT-2004-50600008. Experiments
292 were carried out on the IJL Project TUBE-Davms equipment funded by FEDER (EU), PIA
293 (Programme Investissement d’Avenir), Region Grand Est, Metropole Grand Nancy, and
294 ICEEL.

295

296 The authors have no competing interests to declare

297

298

299 **References:**

300

301 [1] E. Beaupaire, J.-C. Merle, A. Daunois, and J.-Y. Bigot, Phys. Rev. Lett. **76**, 4250 (1996)

302

303 [2] B. Koopmans, G. Malinowski, F. Dalla Longa, D. Steiauf, M. Fähnle, T. Roth, M. Cinchetti,
304 and M. Aeschlimann, Nat. Mater. **9**, 259 (2010)

305

306 [3] M. Battiato, K. Carva, and P. M. Oppeneer, Phys. Rev. Lett. **105**, 027203 (2010)

307

308 [4] K. Carva, M. Battiato, and P. M. Oppeneer, Phys. Rev. Lett. **107**, 207201 (2011)

309

310 [5] S. Essert and H. S. Schneider, J. Appl. Phys. **111**, 07C514 (2012)

311

312 [6] K. Carva, M. Battiato, D. Legut, and P. M. Oppeneer, Phys. Rev. B **87**, 184425 (2013)

313

314 [7] A. J. Schellekens, W. Verhoeven, T. N. Vader, and B. Koopmans, Appl. Phys. Lett. **102**,
315 252408 (2013)

316

317 [8] V. Shokeen, M. Sanchez Piaia, J.-Y. Bigot, T. Müller, P. Elliott, J. K. Dewhurst, S. Sharma,
318 and E. K. U. Gross, Phys. Rev. Lett. **119**, 107203 (2017)

319

320 [9] C. Stamm, T. Kachel, N. Pontius, R. Mitzner, T. Quast, K. Holldack, S. Khan, C. Lupulescu,
321 E. F. Aziz, M. Wiestruck and H.A. Dürr, Nat. Mater. **6**, 740 (2007)

322

323 [10] K. C. Kuiper, G. Malinowski, F. Dalla Longa, and B. Koopmans, J. Appl. Phys. **109**,
324 07D316 (2011)

325

326 [11] T. Roth, A. J. Schellekens, S. Alebrand, O. Schmitt, D. Steil, B. Koopmans, M. Cinchetti,
327 and M. Aeschlimann, Phys. Rev. X **2**, 021006 (2012)

328

329 [12] M. Wietstruk, A. Melnikov, C. Stamm, T. Kachel, N. Pontius, M. Sultan, C. Gahl, M.
330 Weinelt, H. A. Dürr, and U. Bovensiepen, Phys. Rev. Lett. **106**, 127401 (2011)

331
332 [13] M. Sultan, U. Atxitia, A. Melnikov, O. Chubykalo-Fesenko, and U. Bovensiepen, Phys.
333 Rev. B **85**, 184407 (2012)
334
335 [14] A. Eschenlohr, M. Sultan, A. Melnikov, N. Berggaard, J. Wiczorek, T. Kachel, C. Stamm,
336 and U. Bovensiepen, Phys. Rev. B **89**, 214423 (2014)
337
338 [15] B. Frietsch, J. Bowlan, R. Carley, M. Teichmann, S. Wienholdt, D. Hinzke, U. Nowak, K.
339 Carva, P.M. Oppeneer, and M. Weinelt, Nat. Commun. **6**, 8262 (2015)
340
341 [16] L. Rettig, C. Dornes, N. Thielemann-Kühn, N. Pontius, H. Zabel, D. L. Schlagel, T. A.
342 Lograsso, M. Chollet, A. Robert, M. Sikorski, and S. Song, Phys. Rev. Lett. **116**, 257202 (2016)
343
344 [17] O. Chubykalo-Fesenko, U. Nowak, R. W. Chantrell, and D. Garanin, Phys. Rev. B **74**,
345 094436 (2006)
346
347 [18] K. Bobowski, M. Gleich, N. Pontius, C. Schüßler-Langeheine, C. Trabant, M. Wietstruk,
348 B. Frietsch, and M. Weinelt, J. Phys. Condens. Matter **29**, 234003 (2017)
349
350 [19] I. A. Campbell, J. Phys. F Met. Phys. **2**, L47 (1972)
351
352 [20] M. S. S. Brookes, L. Nordström, and B. Johansson, J. Phys. Condens. Matter **3**, 2357
353 (1991)
354
355 [21] I. Radu, K. Vahaplar, C. Stamm, T. Kachel, N. Pontius, H. A. Dürr, T. A. Ostler, J. Barker,
356 R. F. L. Evans, R. W. Chantrell, and A. Tsukamoto, Nature **472**, 205 (2011)
357
358 [22] V. López-Flores, N. Berggaard, V. Halté, C. Stamm, N. Pontius, M. Hehn, E. Otero, E.
359 Beaurepaire, and C. Boeglin, Phys. Rev. B **87**, 214412 (2013)
360
361 [23] C. E. Graves, A. H. Reid, T. Wang, B. Wu, S. de Jong, K. Vahaplar, I. Radu, D. P. Bernstein,
362 M. Messerschmidt, L. Müller, and R. Coffee, Nat. Mater. **12**, 293 (2013)
363
364 [24] N. Berggaard, V. López-Flores, V. Halté, M. Hehn, C. Stamm, N. Pontius, E. Beaurepaire,
365 and C. Boeglin, Nat. Commun. **5**, 3466 (2014)
366
367 [25] I. Radu, C. Stamm, A. Eschenlohr, F. Radu, R. Abrudan, K. Vahaplar, T. Kachel, N. Pontius,
368 R. Mitzner, K. Holldack, and A. Föhlisch, SPIN **5**, 1550004 (2015)
369
370 [26] D. J. Higley, K. Hirsch, G. L. Dakovski, E. Jal, E. Yuan, T. Liu, A. A. Lutman, J. P.
371 MacArthur, E. Arenholz, Z. Chen and G. Coslovich, Rev. Sci. Instrum. **87**, 033110 (2016)
372
373 [27] T. Ferté, N. Berggaard, L. Le Guyader, M. Hehn, G. Malinowski, E. Terrier, E. Otero, K.
374 Holldack, N. Pontuis, and C. Boeglin, Phys. Rev. B **96**, 134303 (2017)
375
376 [28] T. Ferté, N. Berggaard, G. Malinowski, R. Abrudan, T. Kachel, K. Holldack, M. Hehn, and
377 C. Boeglin, Phys. Rev. B **96**, 144427 (2017)
378
379 [29] T. Ferté, N. Berggaard, G. Malinowski, E. Terrier, L. Le Guyader, K. Holldack, M. Hehn,
380 and C. Boeglin, J. Magn. Magn. Mater. **485**, 320 (2019)

381
382 [30] M. Hennecke, I. Radu, R. Abrudan, T. Kachel, K. Holldack, R. Mitzner, A. Tsukamoto,
383 and S. Eisebitt, Phys. Rev. Lett. **122**, 157202 (2019)
384
385 [31] U. Atxitia, P. Nieves, and O. Chubykalo-Fesenko, Phys. Rev. B **86**, 104414 (2012)
386
387 [32] U. Atxitia, J. Barker, R. W. Chantrell, and O. Chubykalo-Fesenko, Phys. Rev. B **89**, 224421
388 (2014).
389
390 [33] R. Moreno, T. A. Ostler, R. W. Chantrell, and O. Chubykalo-Fesenko, Phys. Rev. B **96**,
391 014409 (2017)
392
393 [34] R. Moreno, S. Khmelevskiy, and O. Chubykalo-Fesenko, Phys. Rev. B **99**, 184401 (2019)
394
395 [35] Y. Xu, M. Deb, G. Malinowski, M. Hehn, W. Zhao, and S. Mangin, Adv. Mater. **29**,
396 1703474 (2017)
397
398 [36] S. Iihama, Y. Xu, M. Deb, G. Malinowski, M. Hehn, J. Gorchon, E. E. Fullerton, and S.
399 Mangin, Adv. Mater. **30**, 1804004 (2018)
400
401 [37] K. Holldack, J. Bahrtdt, A. Balzer, U. Bovensiepen, M. Brzhezinskaya, A. Erko, A.
402 Eschenlohr, R. Follath, A. Frisov and W. Frentrup, and L. Le Guyader, J. Synchrotron
403 Radiat. **21**, 1090 (2014)
404
405
406 [38] M. Binder, A. Weber, O. Mosendz, G. Woltersdorf, M. Izquierdo, I. Neudecker, J. R. Dahn,
407 T. D. Hatchard, J.-U. Thiele, C. H. Back, and M.R. Scheinfein, Phys. Rev. B **74**, 134404 (2006)
408
409 [39] C. D. Stanciu, A. V. Kimel, F. Hansteen, A. Tsukamoto, A. Itoh, A. Kirilyuk, and T. Rasing,
410 Phys. Rev. B **73**, 220402 (2006)
411
412 [40] P. Hansen, S. Klahn, C. Clausen, G. Much, and K. Witter, J. Appl. Phys. **69**, 3194 (1991)
413
414 [41] M. Mansuripur and M. Ruane, IEEE Trans. Magn. **22**, 33 (1986)
415
416 [42] N. Berggaard, A. Mougin, M. Izquierdo, E. Fonda, and F. Sirotti, Phys. Rev. B **96**, 064418
417 (2017)
418
419 [43] A. Donges, S. Khmelevskiy, A. Deak, R.-M. Abrudan, D. Schmitz, I. Radu, F. Radu, L.
420 Szunyogh, and U. Nowak, Phys. Rev. B **96**, 024412 (2017)
421
422 [44] C. Boeglin, E. Beaurepaire, V. Halté, V. López-Flores, C. Stamm, N. Pontius, H. A. Dürr,
423 and J.-Y. Bigot, Nature **465**, 458 (2010)
424
425 [45] V. Lopez-Flores, J. Arabski, C. Stamm, V. Halté, N. Pontius, E. Beaurepaire, and C.
426 Boeglin, Phys. Rev. B **86**, 014424 (2012)
427
428 [46] E. Jal, M. Makita, B. Rösner, C. David, F. Nolting, J. Raabe, T. Savchenko, A. Kleibert, F.
429 Capotondi, E. Pedersoli, and L. Raimondi, Phys. Rev. B **99**, 144305 (2019)
430

- 431 [47] B. Frietsch, R. Carley, M. Gleich, M. Teichmann, J. Bowlan, and M. Weinelt, *Jpn. J. Appl.*
432 *Phys.* **55**, 07MD02 (2016)
433
- 434 [48] S.-G Gang, R. Adam, M. Plötzing, M. von Witzleben, C. Weier, U. Parlak, D. E. Bürgler,
435 C. M. Schneider, J. Ruzs, P. Maldonado, and P. M. Oppeneer, *Phys. Rev. B* **97**, 064412 (2018)
436
- 437 [49] R. Gort, K. Bühlmann, S. Däster, G. Salvatella, N. Hartmann, Y. Zemp, S. Hohenstein, C.
438 Stieger, A. Fognini, T. U. Michlmayr, T. Bähler, A. Vaterlaus, and Y. Acremann, *Phys. Rev. Lett.*
439 **121**, 087206 (2018)
440
- 441 [50] E. Turgut, D. Zusin, D. Legut, K. Carva, R. Knut, J. M. Shaw, C. Chen, Z. Tao, H.T.
442 Nembach, T.J. Silva, and S. Mathias,, *Phys. Rev. B* **94**, 220408 (2016)
443
- 444 [51] S. Eich, M. Plötzing, M. Rollinger, S. Emmerich, R. Adam, C. Chen, H.C. Kapteyn, M.
445 M. Murnane, L. Plucinski, D. Steil, and B. Stadtmüller, *Sci. Adv.* **3**, e1602094 (2017)
446
- 447 [52] G.-M. Choi and B.-C. Min, *Phys. Rev. B* **97**, 014410 (2018)
448
- 449 [53] M. Haag, C. Illg, and M. Föhnle, *Phys. Rev. B* **90**, 134410 (2014)
450
- 451 [54] B. Andres, M. Christ, C. Gahl, M. Wietstruk and M. Weinelt, and J. Kirschner, *Phys. Rev.*
452 *Lett.* **115**, 207404 (2015)
453
- 454 [55] E. Iacocca, T.-M. Liu, A. H. Reid, Z. Fu, S. Ruta, P.W. Granitzka, E. Jal, S. Bonetti, A.X.
455 Gray, C.E. Graves, and R. Kukreja,, *Nat. Commun.* **10**, 1756 (2019)
456
- 457 [56] N. Thielemann-Kühn, D. Schick, N. Pontius, C. Trabant, R. Mitzner, K. Holldack, H.
458 Zabel, A. Föhlisch, and C. Chüßler-Langeheine, *Phys. Rev. Lett.* **119**, 197202 (2017)
459
- 460 [57] U. Atxitia, *Phys. Rev. B* **98**, 014417 (2018)
461